EnvironmentAsia

The international journal by the Thai Society of Higher Education Institutes on Environment

Land-Cover Change Detection in a Part of Cameron Highlands, Malaysia Using ETM+ Satellite Imagery and Support Vector Machine (SVM) Algorithm

Ayub Mohammadi[1], Himan Shahabi[2*], and Baharin Bin Ahmad[1]

[1]*Faculty of Built Environment and Surveying, Universiti Teknologi Malaysia, Malaysia*
[2]*Department of Geomorphology, Faculty of Natural Resources, University of Kurdistan, Iran*

*Corresponding author: h.shahabi@uok.ac.ir

Abstract

The importance of the land cover map in many areas including environmental issues, regional planning, sustainable development and many other issues has been considered in the global literature. This study aims to detect land cover changes that occurred in a part of Cameron Highlands, Pahang, Malaysia for a decade between early 2008 until the late 2017. However, in this research Landsat-7 (ETM+) satellite data (2008 and 2017) were acquired and corrected using environment for visualizing images (ENVI) software. Support vector machine (SVM) model was used to classify land covers of both years. Results show that during this period of time forest has underwent considerable changes among all from 49.517532 km^2 in 2008 to just 34.90341 km^2 by the year 2017. The second substantial change belongs to vegetation and florification from 31.265611 km^2 in 2008 to a peak of 42.83176 km^2 by the year 2017. It means that forest mostly have been replaced by vegetation and florification. Furthermore, the overall accuracy and Kappa coefficient using confusion matrix for the year 2008, using support vector machine classification model are 96.4051% and 0.9294, respectively. While these values for the year 2017 are 97.5198% and 0.9674 in order. The current research can be valuable for land cover management in Cameron Highlands by Malaysian policy and decision makers.

Keywords: Remote sensing techniques; Geographical information system; Landsat image; Cameron Highlands

1. Introduction

Land cover change detection have been taken into account as one of the main requirements for variety of purposes, including environmental impact evaluation, spatial development, land use change detection, climate change studies, greenhouse gas inventories and etc. (Wessels *et al*., 2003; Burkhard *et al*., 2012; Zhu and Woodcock, 2014; Gómez *et al*., 2016; Wang *et al*., 2017; Yin *et al*., 2018). Recognizing, quantifying and monitoring changes by remote sensing and geospatial database in any scale and place have been considered in the international literature (Turner *et al*., 2007; Jin *et al*., 2013; Belward and Skøien, 2015; Lv *et al*., 2017;

Ma *et al.*, 2017; Sidhu *et al.*, 2018). However, digital land cover change detection is a process of measuring and extracting the changes that occurred in a specified place through satellite imagery.

Forest losses and its replacement by other land covers is the least well identified and quantified land cover changes and also is one of the main problems worldwide (Chidumayo, 2013; Mayes *et al.*, 2015; Megahed *et al.*, 2015; Miettinen *et al.*, 2016). Malaysia and Cameron Highlands in particular are not exception in this case and have been experienced huge land cover changes. Natural causes are the main reason for long term changes in land cover, however human activities play a substantial role in changing land covers across the world (Jin *et al.*, 2013; Sidhu *et al.*, 2018). As a matter of fact, Cameron Highlands is a tropical area, where most of the time is under the cloud coverage therefore acquiring multispectral images without cloud coverage takes too much time.

Time consuming, expensive and traditional methods of field survey, interpreting old map and literature review are not enough to understand, recognize and quantify the happened changes in predetermined areas like Cameron Highlands. However, remote sensing offers an outstanding tool to measure changes in land covers in different scales, times and places (Moser *et al.*, 2013; Amici *et al.*, 2017; Hasmadi *et al.*, 2017; Wu *et al.*, 2017). The current research is highly useful for policy and decision makers in order to monitor the study area, because it opens up new opportunity of quantifying the changes among different land covers. However, using ETM+ satellite imagery as well as SVM model are the contribution to the knowledge of the current study.

Many studies have been focused on land cover change detection by using different of models, techniques, and satellite imageries, including Shahabi *et al.* (2012) used normalized difference vegetation index (NDVI), principal component analysis (PCA); Nutini *et al.* (2013) employed multi-temporal analysis and Landsat images; Kim *et al.* (2014) used Landsat imageries; Mayes *et al.* (2015) benefited from Landsat 5-8 data and linear spectral mixture analysis; Choudhary and Pathak (2016) examined land use change detection using Landsat imageries of TM. ETM and OLI; Leite *et al.* (2017) utilized Landsat 5/TM images and geographical objects; Sidhu *et al.* (2018) applied the Google Earth for land cover change mapping; Zoungrana *et al.* (2018) employed MODIS satellite imagery for application of land cover change detection.

This study aims to assess and quantify the changes occurred in the land covers from the year 2008 until the late 2017 for a part of Cameron Highlands using support vector machine (SVM) model.
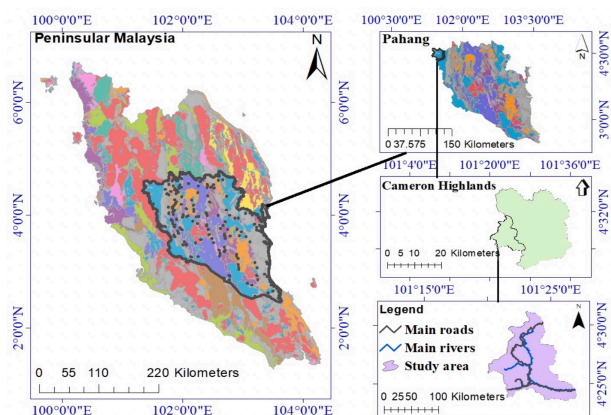
2. Description of the study area

Figure 1. Geographical location of the study area

Table 1. ETM+ spectral bands, bandwidth and ground resolution

Spectral Band	Half-Amplitude Bandwidth (μm)	Sub-satellite Ground Resolution (m)
Panchromatic	0.520±0.010 - 0.900±0.010	13 x 15
1	0.450±0.005 - 0.515±0.005	30
2	0.525±0.005 - 0.605±0.005	30
3	0.630±0.005 - 0.690±0.005	30
4	0.775±0.005 - 0.900±0.005	30
5	1.550±0.010 - 1.750±0.010	30
6	10.40±0.100 - 12.50±0.100	60
7	2.090±0.020 - 2.350±0.020	30

For this study a part of Cameron Highlands, Pahang, Malaysia was selected. However, this scope located in the Longitudes 101˚ 20' 00"E to 101˚ 27' 10"E and Latitudes 4˚ 23' 30" N to 4˚ 31' 10" N. The study area covers 86.895 km² (Figure 1). Cameron Highlands is located in the Main Range of Malaysia geological units, which is narrow and sharply defined (Lee, 2009; Makoundi *et al.*, 2014).

The study area is a farming place and also an attractive tourist destination for people around the world, therefore, it needs fundamental consideration from Malaysian government. The lowest and the highest area in the region are 912 meters and 1960 meters above the sea level. Refer to Malaysian Meteorological Department (MMD) the average rainfall in the study area fluctuates between 1800 mm to 3000 mm annually. In the study area, land covers of florification and forest have the biggest areas of 42.83176 km² and 34.90341 km², respectively.

3. Materials and Methods

In this study the Landsat-7 ETM+ data for a part of Cameron Highlands were downloaded through Earthexplorer.usgs.gov website. Since we determined to detect changes for a decade, then ETM+ data of early 2008 and the late 2017 were collected. Table 1 illustrates the characteristics of ETM+ satellite imagery.

However, these data by using environment for visualizing images (ENVI) software radiometrically, atmospherically, spectrally and geometrically were corrected. Because scan line corrector (SLC) of the Landsat-7 from the year 2003 onward has not been working properly, so all the Landsat-7 data from aforementioned date onward have to be spatially gap filled.

Once the spatial resolution of satellite imageries have been resampled to 15 meters (using panchromatic band), they are then used to generate normalized difference vegetation Index (NDVI) and normalized difference built-up index (NDBI). NDVI map was derived from ETM+ as follows:

$$NDVI = \frac{NIR - Red}{NIR + Red} \tag{1}$$

Where: Near infrared (NIR) band reflects the electromagnetics pulses and Red band absorb them (Zhang *et al.*, 2018). Values of NDVI equation range from − 1 to +1, where positive values show vegetated areas, while negative values implie non-vegetated regions. On the other hand, NDBI is calculated as bellow:

$$NDBI = \frac{SWIR - NIR}{SWIR + NIR} \tag{2}$$

Where: Short-wavelength infrared (SWIR) band is generally sensitive to water and moisture and near infrared (NIR) band reflects the electromagnetics pulses based on the rate of the chlorophyll in vegetation coverage, where the more the chlorophyll the high the reflection will be (Zha *et al.*, 2003). Combination of these two indices with the other bands are highly effective to extract built-up and vegetation land covers.

The SVM is a fast and an accurate model

for the change detection projects (Qi *et al.*, 2013; Rebentrost *et al.*, 2014; Gu and Sheng, 2017). This model provides a good result from noisy and complex data (Gu and Sheng, 2017). It tries to separate the created classes with a decision surface, which maximizes the margin between the selected classes (Qi *et al.*, 2013). Despite this fact that the SVM is a binary classifier, it works as a multiclass classifier as well, provided that several binary SVM classifiers are combined (Steinwart and Christmann, 2008). The SVM classifier runs on the region of interests (ROIs). The classifier performs training at the lower resolution level, because retraining at each level provides higher accuracy for the resampled image, however, it considers the rule image values to identify those that exceed the probability threshold (Steinwart and Christmann, 2008; Gu and Sheng, 2017). It has four types of kernel, including linear, polynomial, radial basis function (RBF), and sigmoid (Hearst *et al.*, 1998). However, the mathematical representation of them is as below:

Linear; $K(X_i X_i) = X_i T X_i$ (3)
Polynomial; $K(X_i X_i) = (g X_i T X_i + r)^d, g>0$ (4)
RBF; $K(X_i X_i) = exp(-g II X_i - X_i II^2), g>0$ (5)
Sigmoid; $K(X_i X_i) = \tanh(g X_i T X_i + r)$ (6)

where g is the gamma term in the all kernels except linear one, d is the polynomial degree in the polynomial kernel, and r is the bias term in the polynomial and sigmoid kernels.

After applying the SVM model we employed post-classification process to delete unwanted pixels the majority and minority filters. As a matter of fact, overusing majority and minority filters result in deleting accurate pixels in the final map, therefore it is necessary to generate segmentation image for those classes that there are unwanted pixels in. Using the decision tree (DT) classifier, both the SVM and the segmentation image were used to produce final raster image (Figure 2). For example, there are a few regions in the final map that classified as water body, which in realty some regions are not water body, however, by applying

segmentation image commend in ENVI software for water body we can easily identify the correct pixel values for water body and assign those pixel values that are not water body to the accurate land cover using DT classifier.

Validation Purposes is an essential step in hazard studies (Stehman, 1997; Beguería, 2006; Hand, 2009; García-Llamas *et al.*, 2018). However, in this study for every land cover 30 ground control points (GCPs) were extracted from the Google Earth image supported by field survey and used for validation purposes by using confusion matrix extension in ENVI software. Overall accuracy is calculated by measuring the number of corrected classified pixels then dividing by the total number of pixels (Jensen and Lulla, 1987). Referring to them, another way to measure the accuracy of classification is the Kappa coefficient, which is calculated via multiplying the total pixels in all the ground truth classes by sum of confusion matrix diagonals then subtracting sum of ground truth pixels in a class times and the sum of classified pixels in that class summed over all classes finally dividing by the entire pixels.

$$OA = \frac{1}{N} \sum P_{ii} \quad (7)$$

Where: OA = Total accuracy, N = Total number of test pixels, and ΣP_{ii} = Total pixels that are correctly classified.

Equation 2 was used for the Kappa coefficient.

$$K = \left(OA - \frac{1}{q}\right)\left(1 - \frac{1}{q}\right) \quad (8)$$

Where: k = kappa coefficient and q = unclassified pixels.

4. Results and Discussion

Using Arc-GIS and Microsoft Excel software the statistical changes for a decade from the year 2008 to the year 2017 in a part of Cameron Highlands were calculated. Table 2 clearly lists the statistical changes occurred in this period of time.

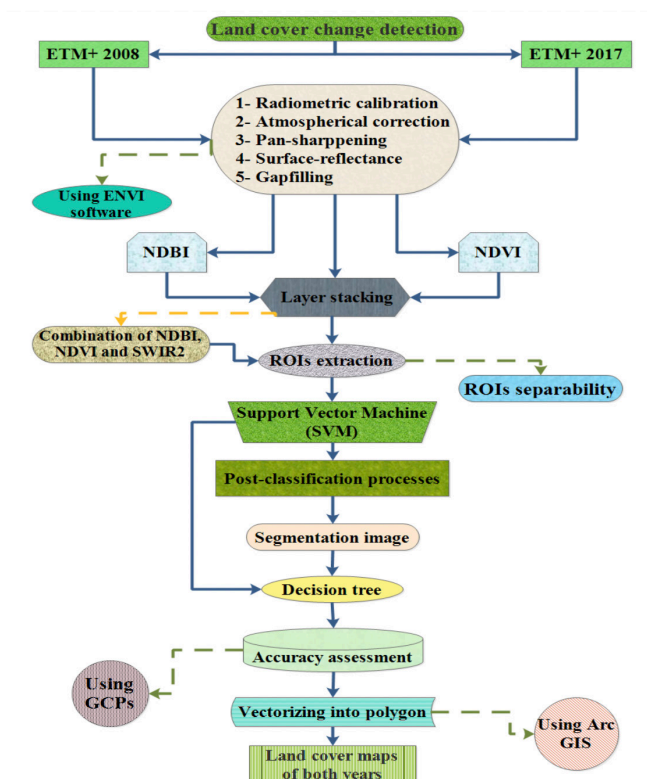Forest have seen the most considerable changes in the study area from 49.517532 km^2 in

Figure 2. Research methodology of the research

Table 2. Statistical changes in a decade (Years 2008 to 2017)

	Year 2008			Year 2017	
No	Name	Area km^2	No	Name	Area km^2
1	Forest	49.517532	1	Forest	34.90341
2	Water body	0.294632	2	Water body	0.364556
3	Tea plantation	3.42952	3	Tea plantation	3.724364
4	Township	2.401528	4	Township	4.639532
5	Vegetation and florification	31.265611	5	Vegetation and florification	42.83176
6	-----------------		6	Cleared forest	0.436157

the year 2008 to 34.90341 km^2 by the year 2017. Vegetation and florification has undergone huge changes from 31.265611 km^2 in the year 2008 to a peak of 42.83176 km^2 by the year 2017. Another remarkable change has occurred for township areas, where it roughly doubled from

2.401528 km^2 in the year 2008 to 4.639532 km^2 in comparison with the year 2017.

Water body has experienced the least positive change of approximately 0.07 km^2 in this decade. About 0.3 km^2 has added to the tea plantation fields in this period of time.
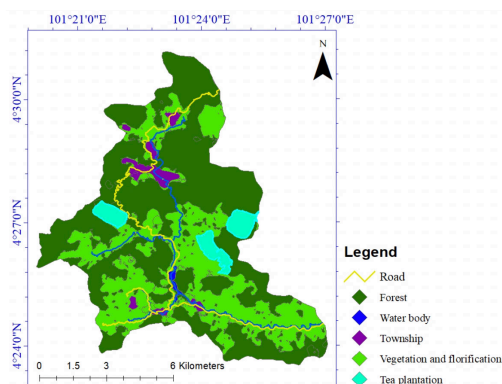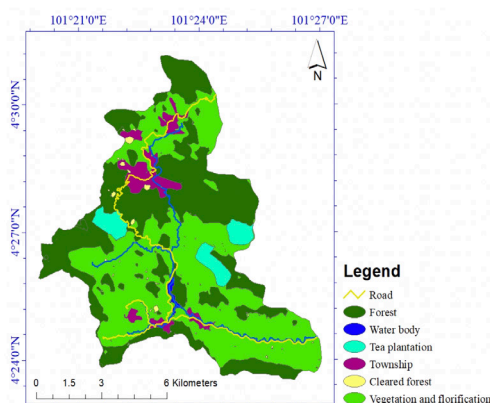
Figure 3. Land cover map of the study area (Year 2008)

Figure 4. Land cover map of the study area (Year 2017)

Table 3. Highlights overall accuracy and Kappa coefficient

Confusion matrix		
	Overall accuracy %	**Kappa coefficient**
Year 2008	96.4051	0.9294
Year 2017	97.5198	0.9674

Eventually, 0.436157 km² as the cleared forest was classified in the year 2017 (Figure 3 & 4).

The overall accuracy and the Kappa coefficient using confusion matrix for either maps were calculated using ENVI software and ground control points (Table 3).

One of the main steps in extracting region of interests (ROIs) is separability evaluation of them (Laurin *et al.*, 2013; Levin, 2016; García-Llamas *et al.*, 2018), because the separability of the ROIs guarantees the validity and reliability of used classification models. The measuring value for ROIs separabilty is between one and two, once it has been upper than 1.8, then the ROIs is acceptable (Laurin *et al.*, 2013). The higher the value the more precise the ROIs will be (Griffiths *et al.*, 2013; Levin, 2016).Table 4 demonstrates the ROIs separability (Least to most) for the either years.

5. Conclusion

Table 4. Region of interests (ROIs) Separability

Year 2008	Year 2017
Tea plantation and vegetation/florification = 1.9591	Tea plantation and vegetation/florification = 1.9614
Forest and vegetation/florification = 1.9680	Township and cleared forest = 1.9706
Forest and tea plantation = 1.9690	Cleared forest and vegetation/florification = 1.9810
Township and vegetation/florification = 1.9789	Township and vegetation/florification = 1.9914
Tea plantation and township = 1.9799	Forest and vegetation/florification = 1.9934
Forest and township = 1.9899	Water body and township = 1.9964
Water body and forest = 1.9959	Water body and vegetation/florification = 1.9978
Water body and tea plantation = 1.9979	Water body and cleared forest = 1.9978
Water body and township = 1.9989	Forest and township = 1.9999
Water body and vegetation/florification = 1.9999	Forest and tea plantation = 1.9999
	Forest and water body = 1.9999
	Tea plantation and cleared forest = 1.9999
	Forest and cleared forest = 1.9999
	Water body and tea plantation = 1.9999
	Tea plantation and township = 1.9999

The current study detected the changes for a decade from early 2008 to the late 2017 in a part of Cameron Highlands, Pahang, Malaysia. We acquired the two Landsat-7 (ETM+) satellite imageries. Once correction process using ENVI software have been completed the NDVI and the NDBI were extracted and stacked with the corrected multispectral bands.

Separability processes were done for the all extracted ROIs from satellite imageries. Using these extracted ROIs the SVM classification model was generated, this model is a fast and an accurate model, by which good results from noisy and complex data can be extracted. The unexpected and unwanted pixels were excluded through post-classification process. Using the DT classifier the information of the SVM model as well as segmentation images were combined for the final maps. By a set of GCPs the final maps were validated through confusion matrix command in ENVI software. Forest areas decreased about 14.61 km^2 by the year 2017 in comparison with the year 2008, while vegetation and florification increased approximately 11.56 km^2 by the year 2017. However, high overall accuracy and Kappa coefficient for both final maps demonstrate that the study well validated.

Overall, we concluded that the introduced method for land cover change detection of part of Cameron Highlands, Malayis is fairly good change detection method can be conservatively suggested for same purposes in other areas. The SVM model can be recommended for land cover change detection areas within the study area. This model can also be introduced as a new encouraging tool for land cover changes evaluation in different similar areas. Our findings can be applied by watershed managers, stakeholders, and land policy makers in order for managing of land cover changing.

Acknowledgement

References

Amici V, Marcantonio M, La Porta N and Rocchini D. A multi-temporal approach in MaxEnt modelling: A new frontier for land use/land cover change detection. Ecological Informatics 2017;40:40-49.

Beguería S. Validation and evaluation of predictive models in hazard assessment and risk management. Natural Hazards. 2006;37(3):315-329.

Belward AS and Skøien JO. Who launched what, when and why; trends in global land-cover observation capacity from civilian earth observation satellites. ISPRS Journal of Photogrammetry and Remote Sensing. 2015;103:115-128.

Burkhard B, Kroll F, Nedkov S and Müller F. Mapping ecosystem service supply, demand and budgets. Ecological Indicators. 2012;21:17-29.

Chidumayo E. Forest degradation and recovery in a miombo woodland landscape in Zambia: 22 years of observations on permanent sample plots. Forest Ecology and Management. 2013;291:154-161.

Choudhary R and Pathak D. Land use/land cover change detection through temporal imageries and its implications in water induced disaster in Triyuga watershed, east Nepal. Journal of Nepal Geological Society. 2016;51:49-54.

García-Llamas P, Geijzendorffer IR, García-Nieto AP, Calvo L, Suárez-Seoane S and Cramer W. Impact of land cover change on ecosystem service supply in mountain systems: a case study in the Cantabrian Mountains (NW of Spain). Regional Environmental Change. 2018:1-14.

Gómez C, White JC and Wulder MA. Optical remotely sensed time series data for land cover classification: A review. ISPRS Journal of Photogrammetry and Remote Sensing. 2016;116:55-72.

Griffiths P, Van Der Linden S, Kuemmerle T and Hostert P. A pixel-based Landsat compositing algorithm for large area land cover mapping. IEEE Journal of Selected Topics in Applied Earth Observations and Remote Sensing. 2013;6(5):2088-2101.

Gu B and Sheng VS. A Robust Regularization Path Algorithm for ν-Support Vector Classification. IEEE Transactions on neural networks and learning systems. 2017;28(5):1241-1248.

Hand DJ. Measuring classifier performance: a coherent alternative to the area under the ROC curve. Machine learning. 2009;77(1):103-123.

Hasmadi M, Pakhriazad H and Shahrin M. Evaluating supervised and unsupervised techniques for land cover mapping using remote sensing data. Geografia-Malaysian Journal of Society and Space. 2017;5(1).

Hearst MA, Dumais ST, Osuna E, Platt J and Scholkopf B. Support vector machines. IEEE Intelligent Systems and their applications. 1998;13(4):18-28.

Jensen JR and Lulla K. Introductory digital image processing: a remote sensing perspective. 1987.

Jin S, Yang L, Danielson P, Homer C, Fry J and Xian G. A comprehensive change detection method for updating the National Land Cover Database to circa 2011. Remote Sensing of Environment. 2013;132:159-175.

Kim D-H, Sexton JO, Noojipady P, Huang C, Anand A, Channan S, Feng M and Townshend JR. Global, Landsat-based forest-cover change from 1990 to 2000. Remote Sensing of Environment. 2014;155:178-193.

Laurin GV, Liesenberg V, Chen Q, Guerriero L, Del Frate F, Bartolini A, Coomes D, Wilebore B, Lindsell J and Valentini R. Optical and SAR sensor synergies for forest and land cover mapping in a tropical site in West Africa. International Journal of Applied Earth Observation and Geoinformation. 2013;21:7-16.

Lee C. Palaeozoic stratigraphy. Geology of Peninsular Malaysia. 2009:55-86.

Leite Lr, Carvalho Lmtd and Silva FMD. Change detection in forests and savannas using statistical analysis based on geographical objects. Boletim de Ciências Geodésicas. 2017;23(2):284-295.

Levin N. Human factors explain the majority of MODIS-derived trends in vegetation cover in Israel: a densely populated country in the eastern Mediterranean. Regional environmental change. 2016;16(4):1197-1211.

Lv Z, Shi W, Zhou X and Benediktsson JA. Semi-automatic system for land cover change detection using bi-temporal remote sensing images. Remote Sensing. 2017;9(11):1112.

Ma L, Li M, Ma X, Cheng L, Du P and Liu Y. A review of supervised object-based land-cover image classification. ISPRS Journal of Photogrammetry and Remote Sensing. 2017;130:277-293.

Makoundi C, Zaw K, Large RR, Meffre S, Lai C-K and Hoe TG. Geology, geochemistry and metallogenesis of the Selinsing gold deposit, central Malaysia. Gondwana Research. 2014;26(1):241-261.

Mayes MT, Mustard JF and Melillo JM. Forest cover change in Miombo Woodlands: modeling land cover of African dry tropical forests with linear spectral mixture analysis. Remote Sensing of Environment. 2015;165:203-215.

Megahed Y, Cabral P, Silva J and Caetano M. Land cover mapping analysis and urban growth modelling using remote sensing techniques in greater Cairo region—Egypt. ISPRS International Journal of Geo-Information. 2015;4(3):1750-1769.

Miettinen J, Shi C and Liew SC. Land cover distribution in the peatlands of Peninsular Malaysia, Sumatra and Borneo in 2015 with changes since 1990. Global Ecology and Conservation. 2016;6:67-78.

Moser G, Serpico SB and Benediktsson JA. Land-cover mapping by Markov modeling of spatial–contextual information in very-high-resolution remote sensing images. Proceedings of the IEEE. 2013;101(3):631-651.

Nutini F, Boschetti M, Brivio P, Bocchi S and Antoninetti M. Land-use and land-cover change detection in a semi-arid area of Niger using multi-temporal analysis of Landsat images. International journal of remote sensing. 2013;34(13):4769-4790.

Qi Z, Tian Y and Shi Y. Robust twin support vector machine for pattern classification. Pattern Recognition. 2013;46(1):305-316.

Rebentrost P, Mohseni M and Lloyd S. Quantum support vector machine for big data classification. Physical review letters. 2014;113(13):130503.

Shahabi H, Ahmad BB, Mokhtari MH and Zadeh MA. Detection of urban irregular development and green space destruction using normalized difference vegetation index (NDVI), principal component analysis (PCA) and post classification methods: a case study of Saqqez City. International Journal of Physical Sciences. 2012;7(17):2587-2595.

Sidhu N, Pebesma E and Câmara G. Using Google Earth Engine to detect land cover change: Singapore as a use case. European Journal of Remote Sensing. 2018;51(1):486-500.

Stehman SV. Selecting and interpreting measures of thematic classification accuracy. Remote sensing of Environment. 1997;62(1):77-89.

Steinwart I and Christmann A. Support vector machines: Springer Science & Business Media; 2008.

Turner BL, Lambin EF and Reenberg A. The emergence of land change science for global environmental change and sustainability. Proceedings of the National Academy of Sciences. 2007;104(52):20666-20671.

Wang B, Choi J, Choi S, Lee S, Wu P and Gao Y. Image fusion-based land cover change detection using multi-temporal high-resolution satellite images. Remote Sensing. 2017;9(8):804.

Wessels KJ, Reyers B, Van Jaarsveld AS and Rutherford MC. Identification of potential conflict areas between land transformation and biodiversity conservation in north-eastern South Africa. Agriculture, ecosystems & environment. 2003;95(1):157-178.

Wu K, Du Q, Wang Y and Yang Y. Supervised sub-pixel mapping for change detection from remotely sensed images with different resolutions. Remote Sensing. 2017;9(3):284.

Yin H, Pflugmacher D, Li A, Li Z and Hostert P. Land use and land cover change in Inner Mongolia-understanding the effects of China's re-vegetation programs. Remote Sensing of Environment. 2018;204:918-930.

Zha Y, Gao J and Ni S. Use of normalized difference built-up index in automatically mapping urban areas from TM imagery. International journal of remote sensing. 2003;24(3):583-594.

Zhang HK, Roy DP, Yan L, Li Z, Huang H, Vermote E, Skakun S and Roger J-C. Characterization of Sentinel-2A and Landsat-8 top of atmosphere, surface, and nadir BRDF adjusted reflectance and NDVI differences. Remote Sensing of Environment. 2018.

Zhu Z and Woodcock CE. Continuous change detection and classification of land cover using all available Landsat data. Remote sensing of Environment. 2014;144:152-171.

Zoungrana BJ, Conrad C, Thiel M, Amekudzi LK and Da ED. MODIS NDVI trends and fractional land cover change for improved assessments of vegetation degradation in Burkina Faso, West Africa. Journal of Arid Environments. 2018;153:66-75.